2016

# Physical and optical properties of phytoplankton-rich layers in a coastal fjord: a step toward prediction and strategic sampling of plankton patchiness

Jason R. Graff
*University of Rhode Island*

Susanne Menden-Deuer
*University of Rhode Island*, smenden@uri.edu



Citation/Publisher Attribution

Graff JR, Menden-Deuer S (2016) Physical and optical properties of phytoplankton-rich layers in a coastal fjord: a step toward prediction and strategic sampling of plankton patchiness. Mar Ecol Prog Ser 544:1-14. https://doi.org/10.3354/meps11601
Available at: https://doi.org/10.3354/meps11601

Vol. 544: 1–14, 2016
doi: 10.3354/meps11601

MARINE ECOLOGY PROGRESS SERIES
Mar Ecol Prog Ser

Published February 18



FEATURE ARTICLE

# Physical and optical properties of phytoplankton-rich layers in a coastal fjord: a step toward prediction and strategic sampling of plankton patchiness

**Jason R. Graff[1,2,*], Susanne Menden-Deuer[1]**

[1]Graduate School of Oceanography, University of Rhode Island, South Ferry Road, Narragansett, RI 02882, USA
[2]*Present address:* Botany and Plant Pathology, Cordley Hall 2082, Oregon State University, Corvallis, OR 97333, USA

ABSTRACT: Dense aggregations of phytoplankton in layers or patches alter the optical and physical properties of the water column and result in significant heterogeneity in trophic and demographic rates of local plankton populations. Determining the factors driving patch formation, persistence, intensity, and dissipation is key to understanding the ramifications of plankton patchiness in marine systems. Regression and multi-parametric statistical analyses were used to identify the physical and optical properties associated with 71 phytoplankton-rich layers (PRLs) identified from 158 CTD profiles collected between 2008 and 2010 in East Sound, Washington, USA. Generalized additive models (GAMs) were used to explore water column properties associated with and characterizing PRLs. Patch presence was associated with increasing water column stability represented by the Brunt-Väisälä frequency ($N^2$), Thorpe scale ($L_t$), and turbulent energy dissipation rate (ε). A predictive regression identified patch presence with 100% accuracy when $\log_{10}(N^2) = -1$ and 70% of the cases when $\log_{10}(\varepsilon) = -3$. A GAM of passively measured variables, which did not include fluorescence, was able to model patch intensity with considerable agreement ($R^2 = 0.58$), and the fit was improved by including fluorescence ($R^2 = 0.69$). Fluorescence alone was an insufficient predictor of PRLs, due in part to the influence of non-photochemical quenching (NPQ) in surface waters and the wide range of fluorescence intensities observed. The results show that a multi-parametric approach was necessary to characterize phytoplankton patches and that physical structure, resulting in steep gradients in bio-optical properties, hold greater predictive power than bio-optical properties alone. Integration of these analytical approaches will aid theoretical studies of phytoplankton patchiness but also improve sampling strategies in the field that utilize autonomous, *in situ* instrumentation.

*Corresponding author: jrgraff@science.oregonstate.edu

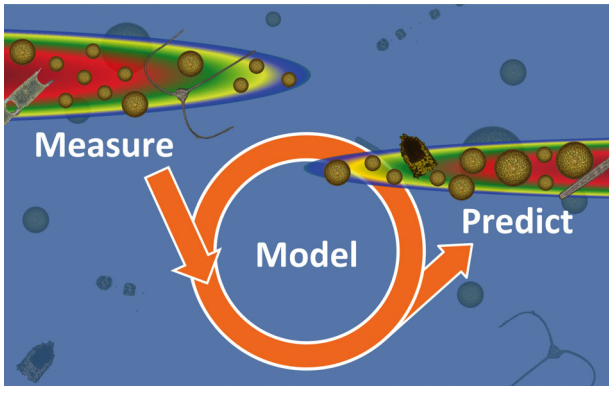


Measuring, modeling, and predicting phytoplankton patches in the coastal ocean.

*Graphic: Jason Graff*

KEY WORDS: Plankton · Patchiness · Water column stability · Fluorescence · Beam attenuation · Generalized additive model · Nonphotochemical quenching

## INTRODUCTION

The heterogeneous nature of plankton distributions have long fascinated and puzzled scientists, including Darwin on the 'Beagle' (Martin 2005). Plankton patches are a visual documentation that assumptions of homogeneity in the marine environment are invalid. Discrete patches with elevated plankton concentrations have important ramifications for the physical, optical and acoustical properties of the water column (reviewed in Durham & Stocker 2012). Plankton patches are characterized by taxonomically diverse communities of auto- and



Publisher: Inter-Research · www.int-res.com

heterotrophic, uni- and multicellular organisms, and, at times, detritus (Alldredge et al. 2002, Rines et al. 2002, Menden-Deuer 2008, Holliday et al. 2010, Rines et al. 2010). Consequently, the mechanisms leading to patch creation are equally diverse. Proposed mechanisms have included physical concentration of cells in areas of neutral buoyancy (Franks & Anderson 1992, Alldredge et al. 2002), shear (Franks 1995, Birch et al. 2008), the balance of phytoplankton growth and zooplankton predation (Menden-Deuer 2008), and swimming behaviors interacting with fluid flow (Bjørnsen & Nielsen 1991, Gallager et al. 2004, Genin et al. 2005, Durham et al. 2009). Measurements of trophic and demographic rates of phytoplankton–zooplankton interactions have shown rapid rates of plankton growth and grazing, which could lead to patch formation and decline on time scales of hours to days (Menden-Deuer & Fredrickson 2010, Menden-Deuer 2012).

A major consequence of plankton patchiness is that biomass and related processes are distributed heterogeneously, providing a challenge for accurately characterizing features of the water column and rate processes. For example in East Sound, Washington, USA, vertically restricted phytoplankton-rich layers (PRLs) occupied <12% of the water column but represented over 50% of the primary production (Menden-Deuer 2012). Rines et al. (2002) showed that the detection of harmful algal bloom (HAB) species depends on the accurate detection of plankton thin layers that could harbor localized concentrations of deleterious species. Accurate identification of patches or layers and the environmental factors leading to their formation is therefore an important prerequisite to advances in passive survey technology and modeling plankton ecology.

Prior investigations of PRLs show that they have unique optical signatures (Donaghay et al. 1992, Cowles & Desiderio 1993). Phytoplankton patches can be horizontally extensive and persist over time scales from hours to several days (Rines et al. 2002, Menden-Deuer 2008), and early investigations suggested that phytoplankton layers are often associated with stratified or vertically stable water columns (Dekshenieks et al. 2001, McManus et al. 2003, Cheriton et al. 2009). Patches or layers composed of photosynthetic plankton are most commonly detected using the *in situ* signal derived from chlorophyll *a* (chl *a*) fluorescence. Using CTD mounted fluorometers, these already-formed patches can be detected and sampled rapidly using optical identification of *in situ* fluorescence profiles (Menden-Deuer 2008, Sullivan et al. 2010b). Although accomplished in real time, this approach to identifying PRLs relies on fortuitous sampling over extensive time and space scales or in places of known patch formation (Dekshenieks et al. 2001, Sullivan et al. 2010a). An alternate approach to PRL identification has been to use airborne lidar for remote detection (Churnside & Donaghay 2009). Airborne surveys vastly increases the spatial scales over which areas can be sampled and the large-scale, long-term processes to which they can be related. Still, subsequent sampling for validation and calibration has to be coordinated with ship-based operations.

Relying solely on optical identification of phytoplankton patches through chl *a* fluorescence signals limits detection of the diverse types of patches that can include non-pigmented particles. More so, patch or PRL detection based on an existing signal limits detection to only those features that have already formed. Field studies can miss the early initiation stages when fluorescence characteristics do not deviate significantly from background values. Consequently, important topics such as patch formation and the evolution of patch or layer characteristics (e.g. optical properties, biological rates) often remain empirically inaccessible. More so, nonphotochemical quenching (NPQ) in phytoplankton (Niyogi et al. 1997, Miloslavina et al. 2009, Milligan et al. 2012), leading to a reduction in measured fluorescence, may alter fluorescence profiles, masking surface layers or falsely indicating a subsurface PRL (Falkowski & Kolber 1995). Photoacclimation to the ambient light regime and pigment regulation due to nutrients could also systematically alter the fluorescence signature of PRL-associated phytoplankton (Menden-Deuer 2012), resulting in an apparent decline or increase in patch intensity. To overcome these obstacles, techniques are needed that allow the detection of diverse PRL types as well as predict the likelihood of future PRL formation and occurrence to facilitate empirical research of plankton patchiness and its ramifications.

Several parameters, beyond fluorescence, are available to characterize plankton patchiness. The concentrated phytoplankton biomass within patches may be detectable through the use of the particulate beam attenuation coefficient ($c_p$; $m^{-1}$). Phytoplankton growth and abundance have been correlated with $c_p$ (Siegel et al. 1989, Durand & Olson 1996, Green et al. 2003, Gernez et al. 2011), and it may serve as a proxy for phytoplankton biomass in the open ocean (Behrenfeld & Boss 2003, 2006). While riverine input and re-suspension of benthic material may alter the par-

ticulate signal in nearshore waters by adding to the total particle field, $c_p$ is most sensitive in the size range ~0.5 to 20 µm (Stramski & Kiefer 1991), which includes most phytoplankton and may provide a useful optical indicator of plankton biomass in coastal seas. Recently, $c_p$ was shown to have a significant relationship with direct measurements of phytoplankton biomass while the particulate backscattering coefficient ($b_{bp}$) showed the strongest correlation with phytoplankton carbon ($C_{phyto}$)(Graff et al. 2015). A proxy such as $c_p$ would provide a convenient means of assessing the carbon dynamics of PRLs in coastal ecosystems, irrespective of phytoplankton photophysiology, when measurements of $b_{bp}$ are not available.

In addition to optical indices, water column stability has been shown to correlate with the presence of phytoplankton thin layers. These parameters include the presence of a strong pycnocline (Dekshenieks et al. 2001) and measures indicative of water column stability, such as a low Brunt-Väisälä frequency, Thorpe scale, and turbulent energy dissipation rate (Cheriton et al. 2009). The specifics of how the relative magnitudes of convergence versus dissipation, by way of shear, buoyancy, motility and turbulence enhanced diffusion balance to drive the shape of a layer's profile are being debated (Stacey et al. 2007, 2009, Birch et al. 2008, 2009) and need to be resolved to gain a mechanistic understanding of plankton patch dynamics.

In the meantime, all of these factors to characterize the physical properties of the water column broaden the parameter space of interest when investigating plankton patchiness and might provide leverage for characterizing the conditions conducive to PRL presence. Predictive algorithms may (1) aid in formulating testable hypotheses about PRL formation and dissipation processes, (2) direct autonomous vehicles based on environmental parameters (e.g. Fiorelli et al. 2003), and (3) lead to the autonomous collection of biological samples and rate measurements (e.g. Pennington et al. 2015). Providing gliders with quantitative observer-independent PRL identification criteria will improve comparability among studies and enable adaptive patch sampling techniques. Adaptive approaches will be necessary to overcome sample size limitations inherent in observation techniques that rely on fortuitous observations of events.

Here, our goal was to develop an empirically based algorithm that would enable the modeling and potential prediction of plankton patchiness based on autonomously acquirable water column characteristics. We used a large data set of water column profiles collected over 3 years in a shallow fjord to determine if we could identify a unique set of parameters to predict (1) plankton patchiness and (2) patch intensity. We found that patch presence may be modeled from water column stability parameters with high accuracy and that patch intensity can be estimated, though less confidently. This approach appears to be a step forward towards predicting and sampling plankton patches and may ultimately serve a critical role in studies of food webs and carbon cycling in the marine environment.

## MATERIALS AND METHODS

### Study site and sampling design

East Sound is a temperate fjord within the San Juan Archipelago in the Northeastern Pacific (48° 38.61′ N, 122° 52.75′ W) (Fig. 1). The fjord extends north–south with a variable width of 1 to 2 km and a maximum depth of 40 m at the most southern end. A partial sill at the southwestern terminus of the fjord restricts circulation and mixing with nearby waters. Day-cruises, 8 in 2008, 6 in 2009, and 10 in 2010 provided the CTD profile library used for our analysis. For each CTD cast, the water column was profiled with a SeaBird 19+ CTD mounted with a

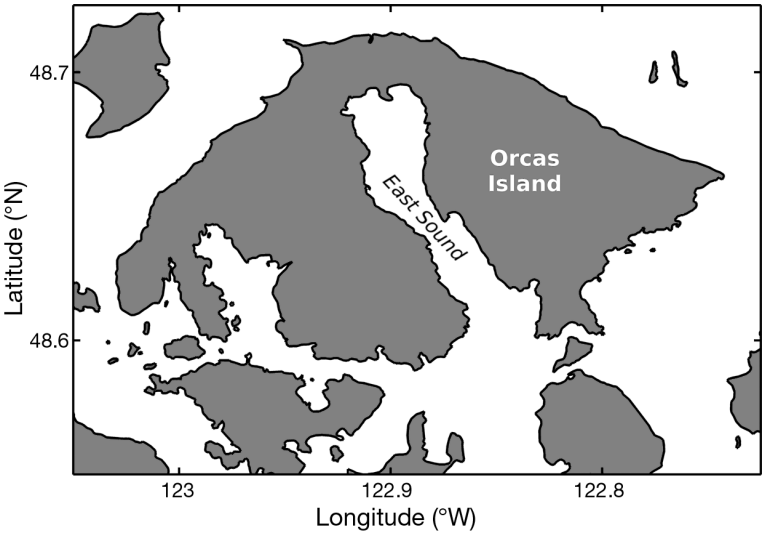


Fig. 1. East Sound in the San Juan Islands, Washington state, USA, Northeast Pacific Ocean

WET Labs WETStar fluorometer, a WET Labs C-Star measuring beam transmission over 25 cm at 660 nm, and a Biospherical QSP-2300L 4π photosynthetically active radiation (PAR) sensor to collect light profiles. The observations of PRLs were evident in repeat casts at the same location, and there was excellent agreement between down- and up-casts. All data presented here were taken from the downcast profiles.

We followed layer identification criteria in Ryan et al. (2008) and Dekshenieks et al. (2001). As such, a profile with a layer was identified based on its fluorescence profile and its maximum had to exceed background values by 3-fold. Background values were calculated as the mean fluorescence outside of 3 m above and below the maximum for the remainder of the water column. To remove a strict restriction as to the maximum vertical extent that could be considered a plankton layer, but often employed for defining phytoplankton 'thin layers', the term 'phytoplankton-rich layers' (PRLs) was used to describe patches of high plankton biomass bordered by steep gradients in plankton concentrations, but criteria regarding the vertical extent of the layers were relaxed (Menden-Deuer 2008). The term PRL is used interchangeably with 'patches' and 'layers' throughout this paper. A steep gradient is the key characteristic of a PRL. Profiles exhibiting high fluorescence values outside of the 3 m above and below the depth of maximum fluorescence were indicative of broad and not steep gradients and were not identified as a patch.

The PRL profiles used in our analysis were collected over multiple years between the months of April and July, and the phytoplankton community composition was taxonomically variable, ranging from highly diverse assemblages to nearly monospecific aggregations of motile and non-motile species (see Menden-Deuer & Fredrickson 2010 for more taxonomic details of patches in East Sound). In the vertical profiles, heterogeneous phytoplankton distributions appear as vertically restricted layers. Through repeat profiling, down to 0.1 nautical miles (nmile; ~185 m) in distance, we found repeat occurrences of PRLs, suggesting that at least some of the features may be horizontally extensive layers, rather than isolated patches. The WETStar fluorometer used in this study was calibrated with discrete samples of extracted chlorophyll and yielded a strong positive correlation between the *in situ* CTD-derived fluorescence and extracted chl *a* (Menden-Deuer 2008, Menden-Deuer & Fredrickson 2010).

### Data handling and statistical analysis

High-resolution data from 158 downcast profiles collected from the CTD package were processed using SeaBird SeaSoft (v. 2). The CTD had an average descent rate of 0.13 m $s^{-1}$ and a sampling rate of 4 Hz. Prior to statistical analyses, the processed data were imported into Matlab (v. 7.4) and depth averaged into 20 cm bins to reduce the effect of infrequent extreme records. This resulted in 11 331 binned observations that were included in the analysis with ~6 observations per depth bin. Beam transmission values were converted to beam attenuation coefficients ($c$) using the equation provided in the WetLabs C-Star manual: $c$ = (−1/beam length) × log(beam transmission). Here we use $c_p'$ instead of the traditional $c_p$ to refer to the particulate beam attenuation coefficient at 660 nm, where $c_p'$ represents particulate beam attenuation values uncorrected for the contribution of pure water and colored dissolved organic matter, with the recognition that the variable constituent of colored dissolved organic matter (CDOM) may influence this analysis (Behrenfeld & Boss 2006). However, at 660 nm, the particulate fraction should dominate the signal, with CDOM being a minor constituent of the measurement (Behrenfeld & Boss 2006). The Brunt-Väisälä frequency ($N^2$; $s^{-2}$), a measure of water column stability, was calculated using the Matlab function sw_bfrq from the SEAWATER (v. 3) package provided by the CSIRO (www.cmar.csiro.au). The Thorpe scale ($L_t$; m), a measure of the length of turbulent overturning events, equals the root mean square displacement of each density measurement based on the reordering of the density profile, where $L_t = (\Delta depth^2/2)^{1/2}$, to make the water column gravitationally stable (Thorpe 1977, Cheriton et al. 2009). The turbulent energy dissipation rate ($\varepsilon = L_t^2 \times N^3$; W $kg^{-1}$) was calculated with the assumption that the Thorpe scale was equal to the Ozmidov scale following similar assumptions and lack of turbulence measurements as in Cheriton et al. (2009). These physical parameters, while not wholly independent, were included in this analysis and each has been previously shown to be correlated with the presence of PRLs (Dekshenieks et al. 2001, Cheriton et al. 2009).

Statistical analyses were performed using Matlab and included regressions of measured and calculated variables, principal component analyses (PCA), and comparisons of physical parameter distributions for patch and non-patch samples, using a 2-sample Kolmogorov-Smirnov (K-S) test. PCA, a method commonly used for data exploration of a large number of

variables that can be difficult to interpret graphically, is the transformation of normalized data onto dimensionally reduced principal component space. The variability of the data along each principal component can be attributed to the contribution of each variable to a principal component. Type II linear regressions were performed for the analysis of *in situ* variables, as each variable was measured with error. Multiple generalized additive models (GAMS) (Hastie & Tibshirani 1986), i.e. linear models composed of a sum contribution of multiple variables, were created to test if patch intensity (PI) of a sample could be estimated from (1) a combination of the variables measured by the CTD package (depth, temperature, salinity, PAR, beam attenuation), with and without fluorescence, or from (2) the variables measured by the CTD package plus the calculated parameters relating to physical properties of the water column (Brunt-Väisälä frequency, Thorpe scale, and turbulent energy dissipation rate). The PI is derived from the fluorescence layer identification criteria (Ryan et al. 2008, Menden-Deuer & Fredrickson 2010) and is calculated as: PI = (Sample fluorescence − Mean background fluorescence)/Maximum fluorescence. Thus, observations within a PRL would generally have PI indices between 0.5 and 1.0, approaching 1.0 in samples with maximum fluorescence. Samples outside a patch have lower values, typically $<0.5$, and falling below zero for samples that have a fluorescence value lower than the mean background fluorescence. The GAMs were created in R (R64.app for Mac OS X GUI 1.36, 5691 Leopard build 64-bit, www.r-project.org). We used the *gam* procedure within the *mgcv* package. This allowed for variables to be non-parametrically estimated smooth functions, potentially going to zero. Allowing for variable functions to approach zero is the equivalent of removing the variable from the model and allows for the elimination of variables that do not improve the fit of the model. We also tested the *step.gam* function (results not shown) but found the *gam* function of the *mgcv* package to provide slightly better approximations of PI based on linear regression analysis of the calculated PI values and model estimated PI values.

Investigations of NPQ were limited to regression analyses and did not include direct physiological measurements on the samples in the field. The analysis included depth-binned regressions of fluorescence (Fl) and $c_p'$ and a regression of Fl normalized to $c_p'$ versus *in situ* PAR. The linear relationship of Fl/$c_p'$ with PAR was fitted with an exponential curve using the *EzyFit* Toolbox (v. 2.41b) for Matlab, by F. Moisy. This fit was used to correct for NPQ by adding the difference between the model and the *y*-intercept to each data point evaluated at its respective *in situ* PAR. The result was then divided by the corresponding $c_p'$ to determine the NPQ-corrected fluorescence.

## RESULTS

Of the 158 profiles, 71 (45%) contained PRLs. Observations from within PRLs accounted for 779 (nearly 7%) of the 11 331 discrete observations. Of the remaining profiles, 68 (43%) contained subsurface fluorescence maxima that occurred over a broad range of depths and thus did not meet our criteria to be identified as PRLs (i.e. mean fluorescence within a patch exceeds background fluorescence by 3-fold). Although not classified as PRLs, the majority of these profiles had heterogeneous, but very broad, fluorescence distributions lacking steep gradients; i.e. fluorescence here should not be assumed to be homogenous (see Fig. 1 in Menden-Deuer [2012] for examples). The remaining 19 (12%) of the profiles had no distinct fluorescence maxima due to uniform fluorescence throughout the entirety of the water column. This range of observations provided suitable controls to test the validity of our predictive algorithm.

Optical measurements of fluorescence and beam attenuation were collected over a wide range of values. *In situ* fluorescence ranged from 0.08 to 4.82 V (instrument range 0−5 V) and beam transmission from 38.9 to 95.7% (instrument range 0−100%), equivalent to $c_p'$ values of 0.17 to 3.77 $m^{-1}$. Regression analysis (Type II) of *in situ* fluorescence and $c_p'$ showed a significant positive correlation ($R^2 = 0.75$, $p < 0.0001$), indicating a strong correspondence between the fluorescence signal (a proxy for chl *a* concentration) and the $c_p'$ signal (a proxy for particulate concentration) (Fig. 2). Non-linear regression did not improve the explanatory power of the regression.

A PCA of the factors distinguishing PRL samples from non-PRL samples indicated that 75.6% of the variability in the data could be explained by a combination of the CTD-measured variables (Fig. 3A). PC1 contributed 39.3% of the explained variability, with temperature and salinity contributing most of the explanatory power. PC2 contributed almost equally (36.3%) to the variability explained, with fluorescence and beam transmission contributing the majority of the explanatory power. PC3, comprised largely of PAR, added a smaller amount of explanatory power (17.3%) and PC4, i.e. exclusively temperature and salinity, even less at 4.7%. The PCA using only the

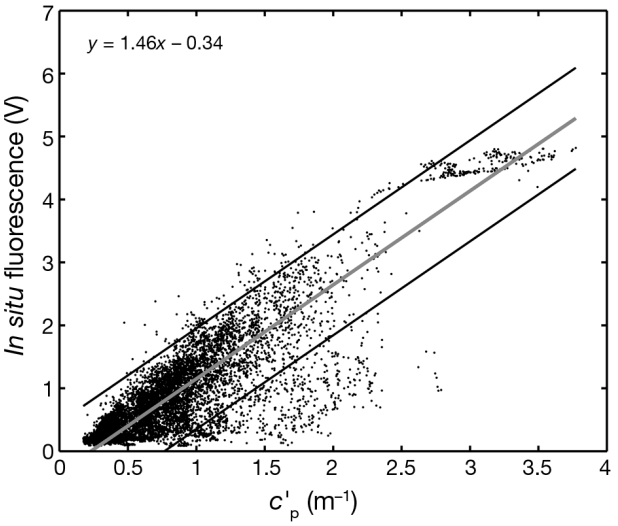


Fig. 2. *In situ* fluorescence (V) versus beam attenuation ($c_p'$, particulate beam attenuation coefficient, $m^{-1}$) for 11 331, 0.2 m depth-binned observations collected from 158 water column profiles. The grey line is a best-fit (Type II) linear regression with the equation shown ($R^2 = 0.75$, $p < 0.0001$). Black lines are the 95% prediction interval for the observations

variables measured by the CTD package did not result in particularly coherent groupings of PRL and non-PRL samples. The inclusion of the physical stability parameters ($N^2$, $L_t$, and ε) in the PCA reduced the explanatory power of the PCA (Fig. 3B) to 54.6% for the first 2 principal components, with PC1 and PC2 contributing 30.0% and 24.6 % of the explained variability, respectively. The turbulent energy dissipation rate (ε) accounted for the second largest portion of the variability on PC1. PC3 and PC4 again contributed a smaller portion of explanatory power at 18.5 and 12.4%, respectively, and were most highly represented by the physical stability parameters. Although the explanatory power was lower, inclusion of the stability parameters improved the distinction between PRL and non-PRL samples (Fig. 3B). This distinction is observed with the PRL samples (black dots in Fig. 3B) forming a cohesive subset within the 'boundaries' of the non-PRL samples (grey dots in Fig. 3B).

A comparison of the frequency distributions of the PRL- and non-PRL-associated stability parameters ($N^2$, $L_t$, and ε) showed that PRLs and non-PRLs could be characterized by significantly different ranges for each parameter. The mean ± SD Brunt-Väisälä frequency for PRL samples was an order of magnitude higher than for non-PRL samples ($N^2 = 0.002 \pm 0.006$ and $N^2 = 0.0005 \pm 0.0016$ $s^{-2}$ in PRL and non-PRL samples, respectively; $p << 0.0001$, KS-test). Similar results were found for mean ε and $L_t$ (Table 1); these being an order of magnitude and a factor of 2 greater in PRL samples, respectively, and coming from significantly different distributions (K-S test, $p << 0.0001$). This characteristic difference in the water column stability parameters between PRL and non-PRL samples provided considerable predictive power for the likelihood of PRL detection (Fig. 4). The probability of an observation being from within a PRL was greatest in stable parts of the water column where

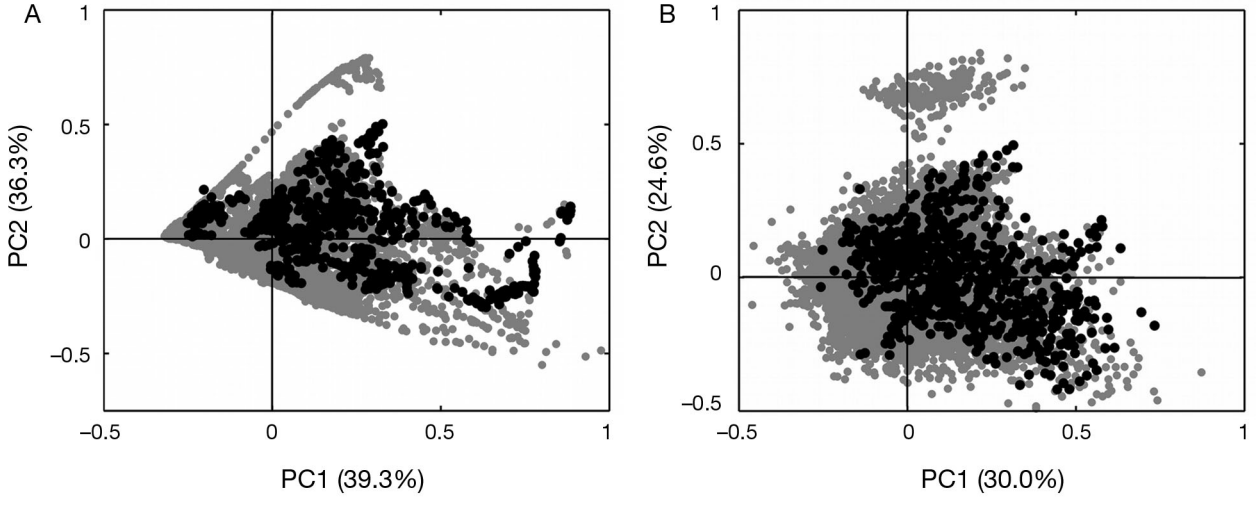


Fig. 3. Principal component analyses of (A) in-water properties: temperature (°C), salinity (psu), photosynthetically active radiation (PAR, µmol photons $m^{-2}$ $s^{-1}$), beam transmission (%), and fluorescence (V); and (B) in-water properties as in panel (A) and including calculated stability parameters: Brunt-Väisälä frequency ($N^2$, $s^{-2}$); Thorpe scale ($L_t$, m); and turbulent energy dissipation rate (ε, W $kg^{-1}$). Including the stability parameters (in B) resulted in a tighter clustering of patch samples (black dots) relative to non-patch samples (grey dots) suggesting that the stability parameters are a unifying characteristic of patches

Table 1. Mean ± SD values of water column physical stability parameters ($N^2$: buoyancy frequency; $L_t$: Thorpe scale; ε: turbulent energy dissipation rate) associated with samples taken when a plankton-rich layer was present (PRL) and not present (non-PRL). Mean values of all 3 parameters are up to an order of magnitude greater for PRL samples than for non-PRL samples. p-values << 0.001 from 2-way Kolmogorov-Smirnov (K-S) tests indicate a significant difference in the distribution of values between PRL and non-PRL samples

| | $N^2$ ($s^{-2}$) | $L_t$ (m) | ε (W $kg^{-1}$) |
|---|---|---|---|
| PRL | 0.002 ± 0.006 | 0.0077 ± 0.016 | $9.12 \times 10^{-7}$ ± 0.006 |
| Non-PRL | 0.0005 ± 0.006 | 0.0044 ± 0.011 | $7.45 \times 10^{-8}$ ± 0.006 |
| p | <<0.001 | <<0.001 | <<0.001 |

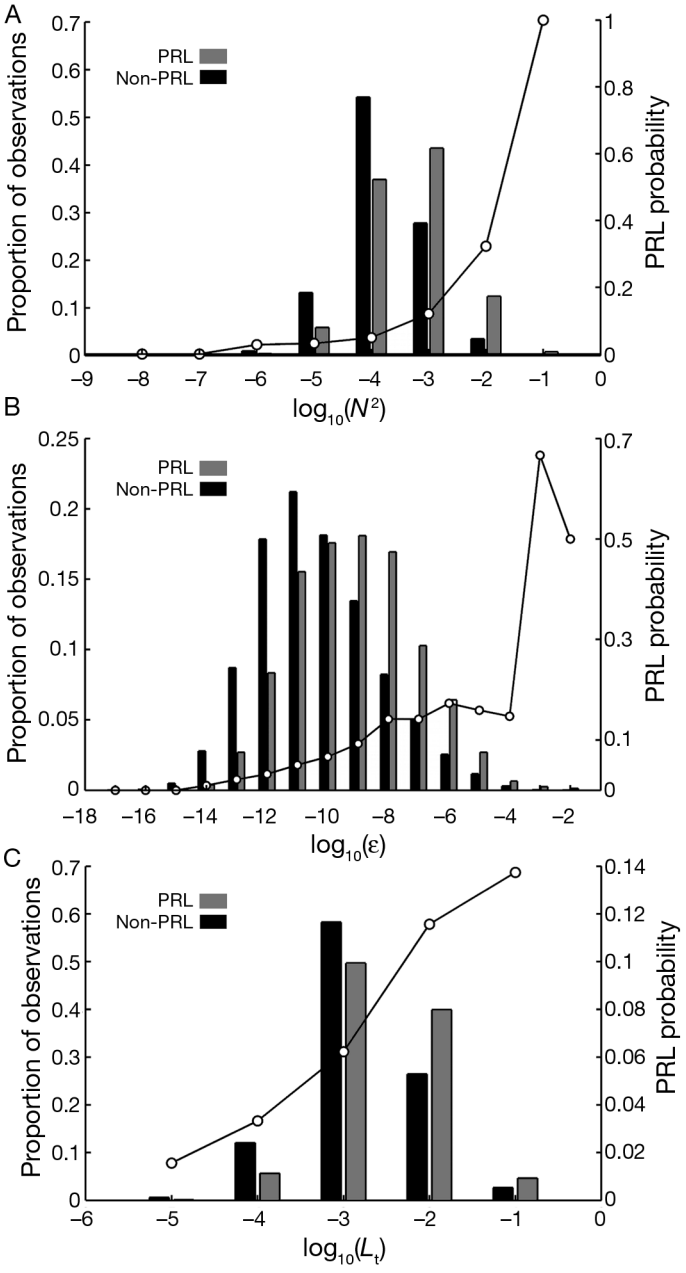


Fig. 4. Normalized histograms of $\log_{10}$-transformed values for (A) the Brunt-Väisälä frequency, ($N^2$, $s^{-2}$), (B) turbulent energy dissipation rate (ε, W $kg^{-1}$), and (C) Thorpe scale ($L_t$, m), for non-patch samples (black) and phytoplankton-rich layer (PRL) only samples (grey), provide the relative frequency of samples in that range of values on the left-hand *y*-axis. The probability (line and circles) of a sample with that particular buoyancy frequency to be within a patch or layer is indicated on the right-hand *y*-axis. Kolmogorov-Smirnoff (K-S) tests of the distributions of patch and non-patch samples for all parameters were significant (p << 0.05). Note the axis ranges

energy dissipation was high and scales of overturning were small. Therefore, water column stability parameters are a necessary addition and provide a significant improvement to predicting patch occurrence and, to a lesser extent, intensity.

Having established the potential for a patch occurrence predictor, we explored characteristics that may provide predictive power of patch intensity. Correlation analyses of the physical stability parameters indicated significant correlations with patch intensity (PI), but the variability explained by these regressions was low ($N^2$: R = 0.17, p < 0.001; ε: R = 0.10, p < 0.001; $L_t$: R = −0.04, p < 0.001). GAMs composed of *in situ* water column properties indicated that a combination of smoothed spline parameters from the CTD provided the best models of PI. Linear regression analysis of the calculated and modeled PI-values using a GAM including fluorescence and a GAM excluding fluorescence produced $R^2$ values of 0.69 and 0.58, respectively (Fig. 5). A smoothed spline of each variable's relative contribution to predicting PI, ranging from < 0 for non-PRL samples to a maximum of 1 for the peak patch intensity, is provided in the right hand panels of Fig. 5, and show the varying combination of each variable to each GAM. While all parameters were considered to be statistically significant to the model, some have a more dynamic contribution over their range of measured values (e.g. fluorescence and beam attenuation) than other variables that had relatively constant contribution over their measured range (e.g. depth and salinity).

The accuracy of the GAMs was assessed by determining the percentage of samples

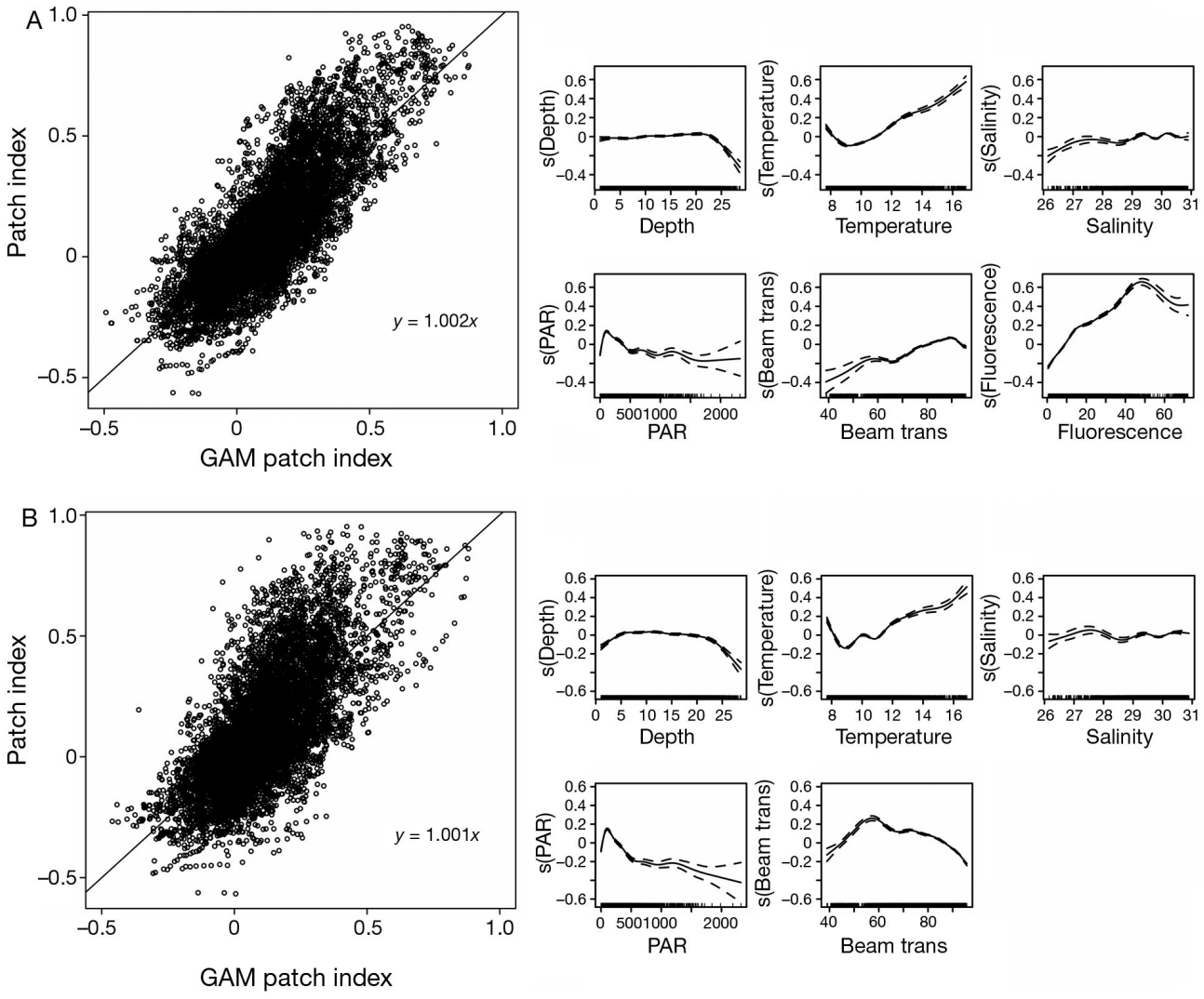


Fig. 5. Regressions of calculated patch intensity (PI) values (large panels) with (A) results from a generalized additive model (GAM) using the input variables: depth, temperature, salinity, photosynthetically active radiation (PAR), beam transmission and fluorescence; $R^2 = 0.68$, and (B) a GAM without fluorescence; $R^2 = 0.58$. A smoothed spline of each variable's relative contribution to predicting PI (black line), ranging from < 0 for non-PRL samples to a maximum of 1 for the peak PI, is provided in the small right-hand panels. Dashed lines are the 95% CI for each spline

with PI ≥ 0.5 that were accurately modeled to have a PI value of that magnitude. The GAM without fluorescence was accurate for 30% of the samples. Including fluorescence in the GAM increased the accuracy to 33%. A GAM consisting of only the Brunt-Väisälä frequency, Thorpe scale, and the turbulent energy dissipation rate ($N^2$, $L_t$, and ε) did a poor job of reproducing PI values ($R^2 = 0.06$, result not shown). Including these parameters in the models along with the CTD parameters did not improve the predictions of PI. Thus, the magnitude of a PRL may be determined using only the parameters most commonly measured by a CTD package.

A comparison of the depths at which the maximum *in situ* fluorescence and maximum $c_p'$ occurred in profiles containing a PRL indicated that these 2 depths did not agree. On average, maximum $c_p'$ occurred 2.1 m above maximum fluorescence. Some of this discrepancy may be due to instances within some profiles of a fresh water lens near the surface carrying a high particulate load of apparently non-fluorescent particles (Fig. 6, above 3 m). However, NPQ could be responsible for some of the differences observed between the depth of maximum $c_p'$ and maximum fluorescence, whether this difference occurred immediately at the surface or at subsurface

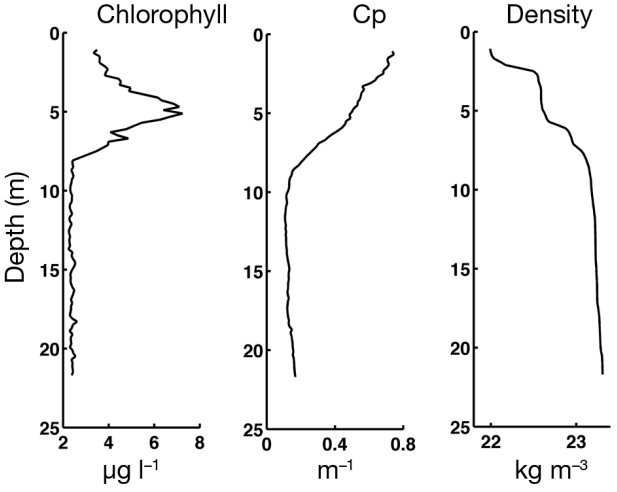


Fig. 6. Example profile of chlorophyll *a*, particulate beam attenuation ($c_p'$), and density for the same vertical profile containing a phytoplankton rich layer in East Sound, WA, USA

depths where irradiance was high at the top of a layer. A regression of $c_p'$ normalized fluorescence (Fl/$c_p'$) versus *in situ* PAR suggests that NPQ was contributing to the offset between max $c_p'$ and Fl (Fig. 7A). In the absence of NPQ, the regression of these parameters would create a horizontal line with slope of zero (dashed line in Fig. 7A). Instead, the results show a decrease in fluorescence per $c_p'$ at higher *in situ* PAR (solid line regression in Fig. 7A). Additionally, depth-binned regressions of Fl and $c_p'$ also suggest NPQ, with lower slopes, i.e. less fluorescence per $c_p'$, in samples at the surface (0–5 m: slope = 0.92; 5–10 m: slope = 1.45; 10–15 m: slope = 1.54) and greater slopes in samples collected in deeper waters (15–20 m: slope = 1.60; 20–25 m: slope = 1.64; 25–30 m: slope = 1.69) (Fig. 7B). An increase of the Fl signal with depth relative to $c_p'$ indicates a masking of Fl in near surface samples.

In order to assess the impact of the potential NPQ on layer detection and patch index values, the exponential regression in Fig. 7A was used to remove the potential contribution of NPQ to fluorescence observations. This was accomplished by adding the difference between the exponential fit evaluated at a given PAR and the *y*-intercept. This correction resulted in the alteration of some fluorescence profiles (Fig. 8). In general, as NPQ was most prevalent in the surface layer, surface fluorescence profiles were most significantly affected. Twelve of the 158 profiles were significantly altered, resulting in the detection of 9 additional PRLs at the surface and altering the profiles such that 3 PRL profiles were reclassified as non-PRL profiles because the fluorescence profile was extended towards the surface. In general, NPQ corrections to the PRL profiles adjusted the depth of maximum fluorescence to become shallower (Fig. 8A), broadened the feature (Fig. 8B), or generated a new PRL where none was previously observed (Fig. 8C). Thus, overall NPQ correction resulted in the detection of additional PRLs. The remaining 92% of all profiles, including PRL profiles, exhibited only small changes.

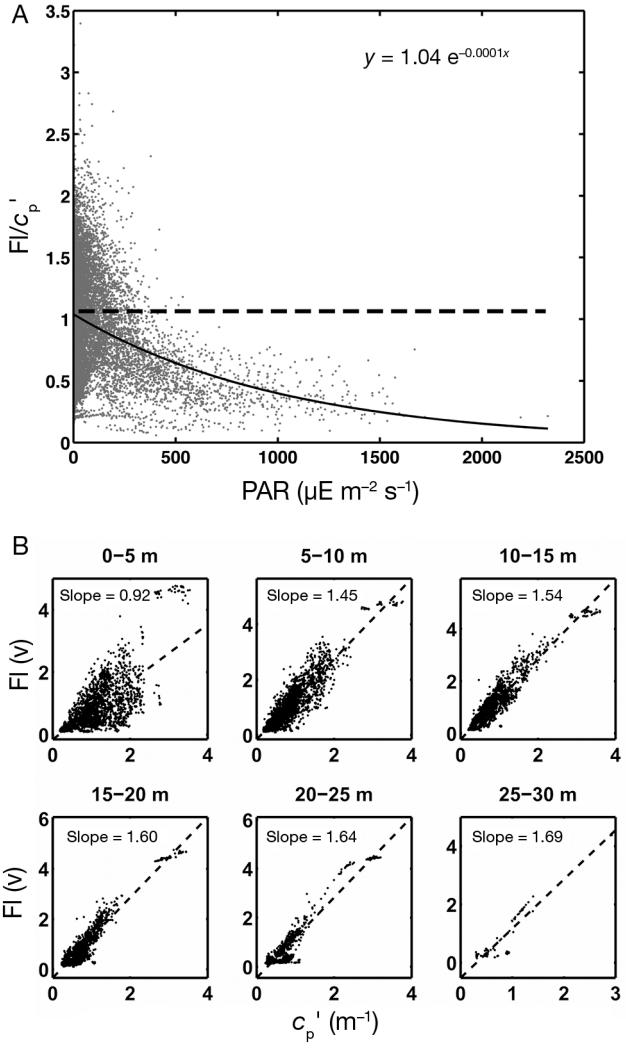


Fig. 7. Possible influence of nonphotochemical quenching (NPQ) from (A) a regression of fluorescence (Fl) normalized to the particulate beam attenuation coefficient (Fl/$c_p'$) versus photosynthetically active radiation (PAR) and (B) 5 m depth-binned regressions of Fl and $c_p'$. In the absence of NPQ or major differences in non-phytoplankton particles, Fl/$c_p'$ should not vary as a function of PAR (dashed line in A) and the slope of Fl versus $c_p'$ would be the same at all depths. The exponential fit $y = 1.04e^{-0.0001x}$ in A was used to correct for NPQ

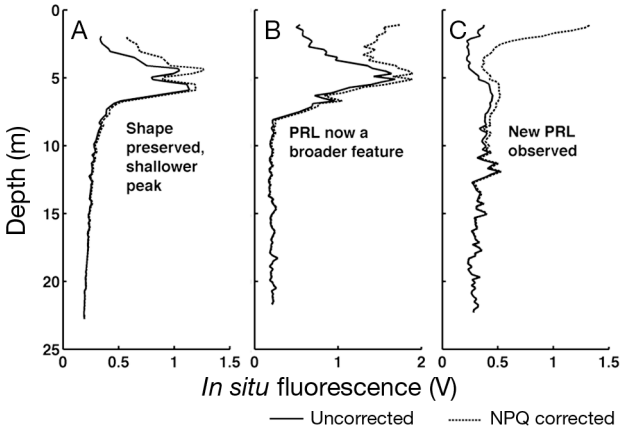


Fig. 8. Example fluorescence profiles before and after applying the correction for non-photochemical quenching (NPQ). (A) The profile of the phytoplankton-rich layer (PRL) remains relatively unchanged with the maximum depth of fluorescence approximately 1.5 m shallower after the correction is applied. (B) The PRL appears as a broader feature after the NPQ correction. (C) Correction results in a newly recognized surface PRL that was not recognized in the uncorrected profile

## DISCUSSION

PRLs can make significant contributions to the productivity and carbon dynamics of coastal waters (Menden-Deuer 2012). Particularly with the advent of broader-scale ocean observation capacity, it is important to evaluate the environmental parameters associated with these patches so they can be detected and their ecology and pervasiveness can be better understood and made accessible to direct sampling, autonomous observations, and modeling efforts. Our analysis revealed that PRL occurrence can be reliably predicted from water column stability parameters despite interannual variability in the water stability parameters and in phytoplankton community composition. Patch intensity, on the other hand, was not related to water column stability and required a complex combination of most of the variables measured by the CTD profiler. It is noteworthy that fluorescence, the parameter previously used to identify PRL presence (e.g. Menden-Deuer 2008) had little predictive power over either patch occurrence or intensity. This is most likely due to differences in the maximum fluorescence of one patch compared to another when analyzed within a large dataset where relatively low values of fluorescence could represent an intense patch due to the even lower background values in the surrounding water column. An approach to identifying and describing patches must include such relative terms in order to be applicable to dynamic datasets collected over large spatial and temporal scales. More so, localized acclimation strategies to the light regime (e.g. NPQ) may significantly alter the detectability and measured intensity of surface patches using *in situ* measurements and, thus, may be an important factor to consider when using remotely sensed data in coastal regions.

The association of PRLs with higher water column stability, particularly with respect to the Brunt-Väisälä frequency, has been observed in prior field studies in Monterey Bay, CA, USA (Dekshenieks et al. 2001, McManus et al. 2005, Cheriton et al. 2009), indicating that our observations in East Sound are not specific to this location. This relationship could potentially be used to predict where layers will form prior to their optical signatures eclipsing those of the surrounding waters. Predicting the occurrence of patches before their formation will be an essential step in Lagrangian studies of patch dynamics to reveal the time-resolved factors driving patch formation. The strong predictive power of patch occurrence through water column stability parameters is indicative that, at least for the patches sampled, physical mechanisms were essential to their formation. While motility could theoretically lead to an aggregation of cells, and thus support patch formation anywhere in the water column, it has been shown that diverse motile plankton respond to physical features through alterations in swimming patterns and growth rates, and thus water column stability may even affect patch formation in motile plankton (Kamykowski 1981, Karp-Boss et al. 2000, Sullivan et al. 2003, Genin et al. 2005, Steinbuck et al. 2009). The majority of patches observed here were dominated by non-motile phytoplankton as described for these patches in Menden-Deuer (2012), suggesting water column stability is even more important to patch formation and persistence by these organisms.

Interestingly, patch intensity had generally low correlation with parameters describing the physical stability of the water column ($N^2$, $L_t$ and ε). Here, it is important to remember that a patch is distributed throughout a range of depths and bordered by steep gradients in relation to a particular measure of stability. Thus, it is difficult to pinpoint a narrow range of parameter values that correspond to high patch intensities, which may explain the lack of correlation. Phytoplankton are exposed to a range of convergence and divergence conditions which influence patch formation and dissipation (Stacey et al. 2007, Birch et al. 2008). In addition to physical mechanisms, biological rates influencing phytoplankton

growth and loss can influence the shape and location of the PRL and its peak (e.g. Benoit-Bird et al. 2009). Thus, it is not necessarily the depth of maximum vertical stratification or stability that determines where the peak of a layer will occur. Nevertheless, the most stable regions of the water column have a higher probability of containing a phytoplankton patch, particularly with respect to the Brunt-Väisälä frequency.

In this study, the intensity (PI) of patches was best modeled by a GAM composed of passively sampled variables including fluorescence, but were modeled almost as well without the use of fluorescence. The model accurately predicted a patch index ≥0.5, 33% of the time when using fluorescence and 30% of the time without this identifying metric. An *a priori* expectation that the inclusion of fluorescence in the GAM, since it was used to calculate the PI, would increase the accuracy of the model more than it did belies the fact that the index used to identify a patch sample represents the ratio of mean water column and peak fluorescence for a particular profile. In other words, the patch index is a relative measure of fluorescence and not an absolute value. A PRL can exist where fluorescence for an entire profile is generally low compared to other profiles but where a peak is present. Conversely, a PRL may not exist where the fluorescence values for the entire water column are extremely high (see Fig. 1 in Menden-Deuer 2012) but lack a significantly distinguishable structure with steep gradients resulting in a peak. Both of these fluorescence patterns were observed and included in the analysis in this study. The strength of the GAM approach, thus, is not due to an inherently circular nature of including fluorescence as a parameter. The complex nature of the fluorescence spline for the GAM using this parameter, in fact, shows the complexity of its usage in the model. Thus, the GAM helps to identify the contribution of multiple parameters to the observation of patchiness, taking into account that their relative contribution might change over the range of values measured. In this case, it showed that while salinity and depth had a constant contribution to the GAM models, fluorescence and beam attenuation were more variable, indicative of a non-linear relationship between patch intensity and the latter 2 variables. Thus, this nonlinearity has to be taken into account when interpreting patchiness. In a practical sense this means that our prior approach of focusing on the fluorescence signal alone is not consistently a reliable contributing variable to identifying patches. This may be subjective to the definition of a patch and may seem intuitive to an observer looking at data in real-time. Reliance on fluorescence must be dampened to some degree as it is not always a strong parameter for modeling purposes, and additional factors will provide additional strength for autonomous platforms to identify where a patch is and, better yet, to predict where a patch might form.

Patches have long been proposed to be trophic hotspots that represent essential resources in an otherwise dilute ocean (Lasker 1975, Mullin & Brooks 1976) and could be an important source of carbon to deeper waters via grazing and sinking mechanisms. This trophic hotspot hypothesis has been empirically verified in East Sound, where measured grazing rates by heterotrophic protists on phytoplankton within patches was significantly higher than outside of patches, with grazers consuming 65% of primary production within patches in comparison to 26% in the remainder of the water column (Menden-Deuer & Fredrickson 2010). Moreover, plankton patches have been identified as production hotspots, where the majority of primary production occurred within patches, which only occupied a small fraction of the water column (Menden-Deuer 2012). Due to the nonlinear dynamics of production and grazing rates, it is challenging to extrapolate bulk rates and plankton dynamics from these heterogeneous measurements. A proxy independent of cellular physiology and relating to phytoplankton carbon, such as the particulate beam attenuation coefficient ($c_p$) or the particulate backscattering coefficient ($b_{bp}$), as demonstrated by Graff et al. (2015) and Behrenfeld & Boss (2003, 2006), may provide a convenient measure of the carbon dynamics of patches over a broad range of spatial and temporal scales. Despite the potentially large variability in the contribution of different particle types to the total particle field in coastal areas (e.g. species composition, freshwater inputs, re-suspension), we found a strong relationship between $c_p'$ and *in situ* fluorescence. The systematic discrepancy between the depth of maximum beam attenuation and maximum *in situ* fluorescence for profiles with patches, however, is a concern for using $c_p$ as a proxy for phytoplankton biomass when investigating surface PRLs. Application of a new method to measure phytoplankton biomass (Graff et al. 2012) has led to advances in relating *in situ* optical properties, specifically the $b_{bp}$ coefficient, to phytoplankton standing stocks (Graff et al. 2015) and could be applied in future studies of patch dynamics and alleviate considerations of phytoplankton photophysiology and its impacts on pigments and fluorescence that are often used in patch identification. However in field studies where $b_{bp}$ is not an available metric, $c_p$ may be a

good alternative (Graff et al. 2015). Combining *in situ* measurement approaches for deteriming phytoplankton biomass with the predictive power of patch occurrence may make studies of plankton population dynamics more accessible and provide much needed data on the relative importance of (1) physical versus biological mechanisms of patch formation, persistence, and decline and (2) overcome obstacles in determining the contribution of plankton patchiness to ecosystem functions.

The divergence in depths of peak values for beam attenuation and fluorescence optical proxies could be due to non-photochemical quenching (NPQ), e.g. photophysiology, depressing fluorescence at shallower depths, or the input of non-chlorophyll-containing particles from nearby coastal sources. We highlight the potential for NPQ in this study and the subsequent effects this has on the interpretation of fluorescence profiles, that is, increasing the overall magnitude of a profile and/or altering the depth of maximum fluorescence, creating a broader structure, or hiding a surface patch completely. Physiological measurements were not collected during these field studies, and as such, the extent to which NPQ was accounted for is our best approximation. From these corrections, only 12 of the 158 PRLs were significantly affected by NPQ, and thus in East Sound it appears to be of minor concern. This is also evident in the robust relationship between extracted chl *a* and fluorescence in East Sound (Menden-Deuer & Fredrickson 2010) which included the extraction of chl *a* from non-PRL samples collected above PRLs where NPQ would be most prevalent. However, more rigorous physiological studies in relation to layer identification and sampling should be performed in the future for more accurate identification of, correction to, and interpretations of patch dynamics when using fluorescence as the optical index for PRLs. This would be particularly helpful during studies following the life history of PRLs that can undergo fluctuations in depth and thus in light exposure and photoacclimation.

## CONCLUSIONS

The ramifications of plankton patchiness for characterizing the optical and acoustical properties of the water column, as well as the quantification of trophic and demographic rates, makes it pertinent that patches are sampled in a deliberate and predictive manner, rather than based on fortuitous observations. The combination of factors identified here as strong predictors of patch occurrence (water column stability) and intensity (CTD-derived measures) makes that goal feasible. The incorporation of physiological measurements to determine the extent of NPQ would also provide evidence for patches in surface waters that may otherwise be missed or undersampled. It is conceivable that water column data from remotely operated or autonomous vehicles, moored profilers, or CTD casts could be input into a predictive model based on methods similar to those presented here. This could include the blending of PCA and regression techniques similar to that provided by partial least squares regression (PLSR). Integration of models like these in autonomous, mobile sampling platforms (e.g. gliders) could ultimately inform the observation and adaptive sampling of patches and direct efforts to locations where patches are likely to form. Future studies that incorporate data from additional regions, seasons, and plankton communities not represented here can test the applicability and reliability of these predictive algorithms across diverse conditions, potentially leading to a robust universal model for identifying and predicting plankton patchiness.

*Acknowledgements*. We thank the faculty and staff at the Shannon Point Marine Center, Western Washington University for their support and hospitality. RV 'Zoea' skippers G. McKeen and N. Schwarck are gratefully acknowledged as well as the many graduate and undergraduate students who have helped with this research. This research was supported through grants from the Office of Naval Research (N000140710136 and N000141010124).

## LITERATURE CITED

Alldredge AL, Cowles TJ, MacIntyre S, Rines JEB and others (2002) Occurrence and mechanisms of formation of a dramatic thin layer of marine snow in a shallow Pacific fjord. Mar Ecol Prog Ser 233:1–12

Behrenfeld MJ, Boss E (2003) The beam attenuation to chlorophyll ratio: an optical index of phytoplankton physiology in the surface ocean? Deep-Sea Res I 50: 1537–1549

Behrenfeld MJ, Boss E (2006) Beam attenuation and chlorophyll concentration as alternative optical indices of phytoplankton biomass. J Mar Res 64:431–451

Benoit-Bird KJ, Cowles TJ, Wingard CE (2009) Edge gradients provide evidence of ecological interactions in planktonic thin layers. Limnol Oceanogr 54:1382–1392

Birch DA, Young WR, Franks PJS (2008) Thin layers of plankton: formation by shear and death by diffusion. Deep-Sea Res I 55:277–295

Birch DA, Young WR, Franks PJS (2009) Plankton layer profiles as determined by shearing, sinking, and swimming. Limnol Oceanogr 54:397–399

Bjørnsen PK, Nielsen TG (1991) Decimeter scale heterogeneity in the plankton during a pycnocline bloom of *Gyrodinium aureolum*. Mar Ecol Prog Ser 73:263–267

Cheriton OM, McManus MA, Stacey MT, Steinbuck JV (2009) Physical and biological controls on the maintenance and dissipation of a thin phytoplankton layer. Mar Ecol Prog Ser 378:55–69

Churnside JH, Donaghay PL (2009) Thin scattering layers observed by airborne lidar. ICES J Mar Sci 66:778–789

Cowles TJ, Desiderio RA (1993) Resolution of biological microstructure through in-situ fluorescence emission spectra. Oceanography 6:105–111

Dekshenieks MM, Donaghay PL, Sullivan JM, Rines JEB, Osborn TR, Twardowski MS (2001) Temporal and spatial occurrence of thin phytoplankton layers in relation to physical processes. Mar Ecol Prog Ser 223:61–71

Donaghay P, Rines H, Sieburth J (1992) Simultaneous sampling of fine scale biological, chemical, and physical structure in stratified waters. Arch Hydrobiol Beihefte 36:97–108

Durand MD, Olson RJ (1996) Contributions of phytoplankton light scattering and cell concentration changes to diel variations in beam attenuation in the equatorial Pacific from flow cytometric measurements of pico-, ultra-, and nanoplankton. Deep-Sea Res II 43:891–906

Durham WM, Stocker R (2012) Thin phytoplankton layers: characteristics, mechanisms, and consequences. Annu Rev Mar Sci 4:177–207

Durham WM, Kessler JO, Stocker R (2009) Disruption of vertical motility by shear triggers formation of thin phytoplankton layers. Science 323:1067–1070

Falkowski P, Kolber Z (1995) Variations in chlorophyll fluorescence yields in phytoplankton in the world oceans. Funct Plant Biol 22:341–355

Fiorelli E, Bhatta P, Leonard NE, Shulman I (2003). Adaptive sampling using feedback control of an autonomous underwater glider fleet. In: Proc 13th Int Symp on Unmanned Untethered Submersible Technology (UUST). www.princeton.edu/~naomi/uust03FBLSp.pdf

Franks PJS (1995) Thin layers of phytoplankton: a model of formation by near-inertial wave shear. Deep-Sea Res I 42:75–91

Franks P, Anderson D (1992) Alongshore transport of a toxic phytoplankton bloom in a buoyancy current: *Alexandrium tamarense* in the Gulf of Maine. Mar Biol 112: 153–164

Gallager SM, Yamazaki H, Davis CS (2004) Contribution of fine-scale vertical structure and swimming behavior to formation of plankton layers on Georges Bank. Mar Ecol Prog Ser 267:27–43

Genin A, Jaffe JS, Reef R, Richter C, Franks PJS (2005) Swimming against the flow: a mechanism of zooplankton aggregation. Science 308:860–862

Gernez P, Antoine D, Huot Y (2011) Diel cycles of the particulate beam attenuation coefficient under varying trophic conditions in the northwestern Mediterranean Sea: observations and modeling. Limnol Oceanogr 56:17–36

Graff JR, Milligan AJ, Behrenfeld MJ (2012) The measurement of phytoplankton biomass using flow-cytometric sorting and elemental analysis of carbon. Limnol Oceanogr Methods 10:910–920

Graff JR, Westberry TK, Milligan AJ, Brown MB and others (2015) Analytical phytoplankton carbon measurements spanning diverse ecosystems. Deep-Sea Res I 102:16–25

Green RE, Sosik HM, Olson RJ, DuRand MD (2003) Flow cytometric determination of size and complex refractive index for marine particles: comparison with independent and bulk estimates. Appl Opt 42:526–541

Hastie T, Tibshirani R (1986) Generalized additive models. Stat Sci 1:297–310

Holliday DV, Greenlaw CF, Donaghay PL (2010) Acoustic scattering in the coastal ocean at Monterey Bay, CA, USA: fine-scale vertical structures. Cont Shelf Res 30: 81–103

Kamykowski D (1981) Laboratory experiments on the diurnal vertical migration of marine dinoflagellates through temperature gradients. Mar Biol 62:57–64

Karp-Boss L, Boss E, Jumars PA (2000) Motion of dinoflagellates in simple shear flow. Limnol Oceanogr 45: 1594–1602

Lasker R (1975) Field criteria for survival of anchovy larvae — relation between inshore chlorophyll maximum layers and successful first feeding. Fish Bull 73:453–462

Martin A (2005) The kaleidoscope ocean. Philos Trans R Soc A 363:2873–2890

McManus MA, Alldredge AL, Barnard AH, Boss E and others (2003) Characteristics, distribution and persistence of thin layers over a 48 hour period. Mar Ecol Prog Ser 261:1–19

McManus MA, Cheriton OM, Drake PJ, Holliday DV, Storlazzi CD, Donaghay PL, Greenlaw CF (2005) Effects of physical processes on structure and transport of thin zooplankton layers in the coastal ocean. Mar Ecol Prog Ser 301:199–215

Menden-Deuer S (2008) Spatial and temporal characteristics of plankton-rich layers in a shallow, temperate fjord. Mar Ecol Prog Ser 355:21–30

Menden-Deuer S (2012) Structure-dependent phytoplankton photosynthesis and production rates: implications for the formation, maintenance, and decline of plankton patches. Mar Ecol Prog Ser 468:15–30

Menden-Deuer S, Fredrickson K (2010) Structure-dependent, protistan grazing and its implication for the formation, maintenance and decline of plankton patches. Mar Ecol Prog Ser 420:57–71

Milligan AJ, Aparicio UA, Behrenfeld MJ (2012) Fluorescence and nonphotochemical quenching responses to simulated vertical mixing in the marine diatom *Thalassiosira weissflogii*. Mar Ecol Prog Ser 448:67–78

Miloslavina Y, Grouneva I, Lambrev PH, Lepetit B, Goss R, Wilhelm C, Holzwarth AR (2009) Ultrafast fluorescence study on the location and mechanism of non-photochemical quenching in diatoms. Biochim Biophys Acta 1787: 1189–1197

Mullin MM, Brooks ER (1976) Some consequences of distributional heterogeneity of phytoplankton and zooplankton. Limnol Oceanogr 21:784–796

Niyogi KK, Bjorkman O, Grossman AR (1997) *Chlamydomonas* xanthophyll cycle mutants identified by video imaging of chlorophyll fluorescence quenching. Plant Cell 9:1369–1380

Pennington JT, Blum M, Chavez FP (2016) Seawater sampling by an autonomous underwater vehicle: 'Gulper' sample validation for nitrate, chlorophyll, phytoplankton, and primary production. Limnol Oceanogr Methods 14: 14–23

Rines JEB, Donaghay PL, Dekshenieks MM, Sullivan JM, Twardowski MS (2002) Thin layers and camouflage: hidden *Pseudo-nitzschia* spp. (Bacillariophyceae) populations in a fjord in the San Juan Islands, Washington, USA. Mar Ecol Prog Ser 225:123–137

Rines JEB, McFarland M, Donaghay P, Sullivan J (2010) Thin layers and species-specific characterization of the

phytoplankton community in Monterey Bay, California, USA. Cont Shelf Res 30:66–80

Ryan JP, McManus MA, Paduan JD, Chavez FP (2008) Phytoplankton thin layers caused by shear in frontal zones of a coastal upwelling system. Mar Ecol Prog Ser 354:21–34

Siegel DA, Dickey TD, Washburn L, Hamilton MK, Mitchell BG (1989) Optical determination of particulate abundance and production variations in the oligotrophic ocean. Deep-Sea Res 36:211–222

Stacey MT, McManus MA, Steinbuck JV (2007) Convergences and divergences and thin layer formation and maintenance. Limnol Oceanogr 52:1523–1532

Stacey M, McManus M, Steinbuck J (2009) Response to 'Plankton layer profiles as determined by shearing, sinking, and swimming' by D. A. Birch, W. R. Young, and P. J. S. Franks. Limnol Oceanogr 54:400

Steinbuck JV, Stacey MT, McManus MA, Cheriton OM, Ryan JP (2009) Observations of turbulent mixing in a phytoplankton thin layer: implications for formation, maintenance, and breakdown. Limnol Oceanogr 54: 1353–1368

Stramski D, Kiefer DA (1991) Light scattering by microorganisms in the open ocean. Prog Oceanogr 28:343–383

Sullivan JM, Swift E, Donaghay PL, Rines JE (2003) Small-scale turbulence affects the division rate and morphology of two red-tide dinoflagellates. Harmful Algae 2:183–199

Sullivan JM, Donaghay PL, Rines JEB (2010a) Coastal thin layer dynamics: consequences to biology and optics. Cont Shelf Res 30:50–65

Sullivan JM, Van Holliday D, McFarland M, McManus MA and others (2010b) Layered organization in the coastal ocean: an introduction to planktonic thin layers and the LOCO project. Cont Shelf Res 30:1–6

Thorpe S (1977) Turbulence and mixing in a Scottish loch. Philos Trans R Soc A 286:125–181

*Editorial responsibility: Steven Lohrenz, New Bedford, Massachusetts, USA*

*Submitted: May 8, 2015; Accepted: December 30, 2015*
*Proofs received from author(s): February 15, 2016*